

Base Complementarity and Nucleoside Recognition in Phosphatidyl nucleoside Vesicles

Debora Berti and Piero Baglioni*

Department of Chemistry, University of Florence, Via G. Capponi 9, I-50121 Florence, Italy

Silvio Bonaccio, Gabriella Barsacchi-Bo, and Pier Luigi Luisi*

Institut für Polymere, ETH Zentrum, 6 Universitätstrasse, CH-8092 Zürich, Switzerland

Received: September 10, 1997[®]

Phosphatidyl nucleosides that self-assemble in water to form closed liposomes have been investigated by spectroscopic methods to detect whether complementary base recognition can be achieved in spherical bilayer structures. We have prepared and characterized liposomes from 5'-(1,2-dioleoyl-*sn*-glycero(3)phospho)-adenosine (DOP-Ade), 5'-(1,2-dioleoyl-*sn*-glycero(3)phospho)uridine (DOP-Uri), 5'-(1,2-dioleoyl-*sn*-glycero(3)phospho)cytidine (DOP-Cyt), their mixtures, and liposomes formed by 5'-(1-palmitoyl-2-oleoyl-*sn*-glycero(3)phospho)adenosine (POP-Ade) or 5'-(1-palmitoyl-2-oleoyl-*sn*-glycero(3)phospho)uridine (POP-Uri). The 1:1 mixture of DOP-Ade and DOP-Uri liposomal solutions shows UV absorption and circular dichroism properties characteristic for base pairing, since a hypochromic effect, detected in the absorption region of the aromatic bases, is coupled to a CD intensity increase of the same band. The same effect is detected for POP-Ade liposomes mixed with POP-Uri liposomes. The hypochromic effect can be observed after three days from the mixing, and the spectroscopic feature is the same as that observed for freshly prepared liposomes formed by the mechanical 1:1 mixture of the two complementary lipids. Liposomes formed from noncomplementary phosphatidyl nucleosides, i.e. DOP-Ade and DOP-Cyt, fail to give these spectroscopic changes, supporting a specific and stoichiometric base interaction governed by Watson–Crick complementarity. The possible relevance for the origin of life of this recognition mechanism, involving bilayer self-assembling structures, is discussed.

Introduction

The information and self-replication mechanism of DNA and RNA resides on the high sequential and stereochemical order of these macromolecules. An interesting question is whether more primitive structures containing the same bases of RNA or DNA can display similar chemical recognition patterns based on Watson–Crick complementarity. Molecular recognition is a fundamental characteristic of living systems, and much effort has been therefore devoted to achieve selective recognition and binding in artificial systems.

Experimental and theoretical studies on complementary base recognition have been performed in noncompetitive solvents, i.e. organic solvents, while in an aqueous environment stacked structures are more stable than hydrogen-bonded ones.^{1–9} Molecular organization seems to be a necessary requisite for molecular devices that recognize each other through H-bonding in aqueous systems.

The most correct approach to mimic and model molecular recognition through hydrogen bonding in aqueous environment resides in the anchoring of the base moieties to a self-organized supramolecular array, where stacking between the π -electron can contribute to the stabilization of the base complex. This is the mechanism operating for nucleic acids in living systems, where bases are embedded in a linear array and molecular recognition is achieved through a cooperative action, the “zipper effect”.^{7–9}

The PNA (peptide nucleic acid¹⁰) method, where nucleic acid bases are embedded in a polypeptidic chain, is one possible

approach to this research field. Another way to match these functionalities is related to supramolecular devices that can mimic molecular supraorganization and compartmentalization through noncovalent interactions.^{11–15}

Within this field, which has recently been attracting enormous interest, a specific interaction among bases has been reported for thymine derivatives in aqueous micelles.¹⁶ However base pairing occurs even in this case in the hydrophobic core of the micelle, overcoming the competition of the protic solvent by compartmentalization of the partners into the micellar hydrophobic core.

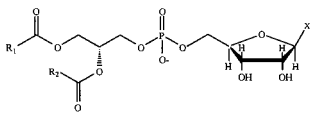
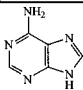
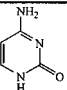
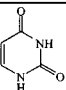
Another possible approach is offered by lipid monolayers and bilayers, whose supramolecular architecture has been widely exploited in membrane mimetic chemistry. Kunitake et al.^{17–19} and Ringsdorf et al.²⁰ have recently reported the surface behavior of some synthetic amphiphiles containing properly functionalized headgroups that display molecular recognition via noncovalent multifunctional interactions, such as hydrogen bonds and hydrophobic and electrostatic interactions. Particularly interesting is the experimental evidence for molecular recognition of nucleotides driven by electrostatic and specific binding by the guanidinium cation at the surface of monolayers, aqueous micelles, and bilayers.²¹ Molecular recognition is deeply affected by the interfacial binding environment, being meaningfully higher for monolayers than for micelles and bilayers. The driving force of the substrate–receptor recognition is represented by the electrostatic interaction between the oppositely charged cationic guanidinium headgroups and the anionic phosphate groups of the base.

We present here experimental evidence for molecular recognition by synthetic amphiphiles that can be enzymatically synthesized from natural substrates, namely phosphocholine and

* Correspondence to this author. Voice: +39.55.2757567. Fax: +39.55.240865. E-mail: colloid@sirio.cineca.it.

[®] Abstract published in *Advance ACS Abstracts*, December 1, 1997.

TABLE 1: Chemical Structure of the Phosphatidyl Nucleosides Reported in This Study

			
Alkyl Chain	X= Base	Name	
R ₁ =Oleoyl	R ₂ =Oleoyl	Adenine	DOP-Ade, 1
R ₁ =Oleoyl	R ₂ =Oleoyl	Uracil	DOP-Uri, 2
R ₁ =Oleoyl	R ₂ =Oleoyl	Cytosine	DOP-Cyt, 3
R ₁ =Palmitoyl	R ₂ =Oleoyl	Adenine	POP-Ade, 4
R ₁ =Palmitoyl	R ₂ =Oleoyl	Uracil	POP-Uri, 5
<div style="display: flex; justify-content: space-around; align-items: center;"> <div style="text-align: center;">  Adenine </div> <div style="text-align: center;">  Cytosine </div> <div style="text-align: center;">  Uracil </div> </div>			

nucleosides. Our aim was to join the self-assembling properties of phospholipids to the molecular recognition properties of nucleic bases.^{22,23} The phosphate group present on the polar head reproduces the structural motif of nucleic acids. It is important to underline that both partners are negatively charged and favorable electrostatic interactions to the binding and recognition process can be ruled out.

Previously it has been reported by us that attractive interactions occur between the complementary nucleobases DOP-Ade and DOP-Uri at the water/air interface only when the subphase is maintained at physiological pH. This attractive behavior cannot be observed in monolayers obtained from the mixture of DOP-Ade and DOP-Cyt, i.e. noncomplementary bases.²³ In this study we extend the previous results to vesicles, which represent a more interesting system because of the cell-like compartmented structure of the vesicle and the possibility of direct spectroscopic observation of the recognition mechanism.

Experimental Section

Materials. 1,2-Dioleoyl-*sn*-glycero(3)-phosphocholine (DOPC), and 1-palmitoyl-2-oleoyl-*sn*-glycero(3)-phosphocholine (POPC) were purchased from Northern Lipids (Canada) and Avanti Polar Lipids (U.S.A.), respectively. Adenosine, uridine, and cytidine were obtained from Fluka (Switzerland). Phospholipase D from *Streptomyces* sp. AA 586 was purchased from Genzyme Diagnostics, West Malling, U.K. Water was purified with a MilliRo/Milliq apparatus. TRIS base, TRIS hydrochloride, and NaCl were purchased from Fluka and used without further purification. 1-*O*-*n*-octyl- β -D-glucopyranoside was obtained from Fluka and used as received.

Synthesis of Phosphatidyl nucleosides. The structure of the phosphatidyl nucleosides, dioleoylphosphatidyladenosine (DOP-Ade), dioleoylphosphatidyluridine (DOP-Uri), dioleoylphosphatidylcytidine (DOP-Cyt), palmitoyl-oleoylphosphatidyladenosine (POP-Ade), and palmitoyl-oleoylphosphatidyluridine (POP-Uri) and are schematically reported in Table 1.

Phosphatidyl nucleosides, 5'-(1,2-dioleoyl-*sn*-glycero(3)-phospho)adenosine (DOP-Ade, **1**), 5'-(1,2-dioleoyl-*sn*-glycero(3)-phospho)uridine (DOP-Uri, **2**), and 5'-(1,2-dioleoyl-*sn*-glycero(3)-phospho)cytidine (DOP-Cyt, **3**), as well as 5'-(1-palmitoyl-2-oleoyl-*sn*-glycero(3)-phospho)adenosine (POP-Ade, **4**) and 5'-(1-palmitoyl-2-oleoyl-*sn*-glycero(3)-phospho)uridine (POP-Uri, **5**), have been synthesized enzymatically in a two-phase CHCl₃/

H₂O system from 1,2-dioleoyl-*sn*-glycero(3)-phosphocholine and adenosine, uridine, and cytidine as described for a variety of other phosphatidyl nucleosides by Shuto et al.^{24–26} following the modifications described by Bonaccio et al.^{27,28} Phospholipase D from *Streptomyces* sp. AA 586 (500–600 units) was used as a catalyst for the transphosphatidylation.

¹H, ³¹P{¹H}, and ¹³C{¹H} NMR spectra were recorded at 500.132, 202.46, and 125.76 MHz, respectively, on a Bruker Avance DRX-500 spectrometer equipped with a variable temperature control unit accurate to ± 0.1 °C. Chemical shifts are relative to tetramethylsilane and to 85% H₃PO₄, respectively, as external references. Downfield values are reported as positive. Double-quantum-filtered ¹H COSY experiments²⁹ were recorded using degassed nonspinning samples with 1024 increments of size 2K covering the full range (ca. 5000 Hz) in both dimensions.

TLC, UV, and NMR data of the phospholiponucleosides are reported in the Appendix.

Vesicle Preparation and Spectroscopic Characterization. Multilamellar vesicles (2.9–3.3 mM total lipid concentration) have been prepared as described earlier³ by dispersing a dry lipid film in the buffer (30 mM Tris, pH 7.5, 20 mM NaCl). These lipids spontaneously form in water polydisperse vesicular suspensions by simple shaking. However in this work the dispersion was sized down to unilamellar vesicles of approximately 33 nm radius by repeated extrusion, at room temperature, of multilamellar liposomes through two stacked polycarbonate membranes with a pore size of 200 nm, followed by extrusion through 100 nm and finally 50 nm pore size membranes.²⁸ Filtration was performed with The Extruder by Lipex Biomembranes, Vancouver (Canada), and Nuclepore polycarbonate membranes. This allows a narrow and reproducible size distribution.

Samples for freeze fracture electron microscopy were cryo-fixed by the propane-jet technique³⁰ and fractured at 108 K in a Balzen BAF 300 at 10^{–5} Pa. Pt/carbon replicas were examined with Philips EM 301 operating at 100 kV.

QELS experiments were carried out on a Brookhaven Instruments apparatus (BI 9000AT correlator and BI 200 SM goniometer). The signal was detected by an EMI 9863B/350 photomultiplier. The light source was a Coherent Innova 90 Ar⁺ laser, at $\lambda = 514$ nm, linearly polarized in the vertical direction, with a power attenuated in order to avoid sample heating. The laser long-term power stability was $\pm 0.5\%$. Homodyne detection was recorded using decahydronaphthalene as cell matching liquid. The data were collected in multiple-sample time detection, and the autocorrelation function of the scattered light intensity was expanded about an average linewidth Γ as a polynomial function of the sample time with cumulants as parameters to be fitted, stopped to the second moment. A weighed least-squares technique was applied to the second-order polynomial function to determine the constants and their standard deviation.

Circular dichroism (CD) measurements were carried out on a JASCO J-600 spectropolarimeter, using a 0.05 cm path length Hellma 121.000 quartz Suprasil cell. Ellipticities, $[\Theta]$, are expressed as molar ellipticities, referred to the total lipid concentration. UV measurements were carried out on Perkin Elmer LAMBDA 5 spectrophotometer using a 0.1 cm path length Hellma 110 quartz Suprasil cell.

The light scattering contribution to the UV absorption spectra was evaluated by polynomial fitting of the absorption curve in the spectral region between 500 and 320 nm, where no absorption from the bases is expected, according to the

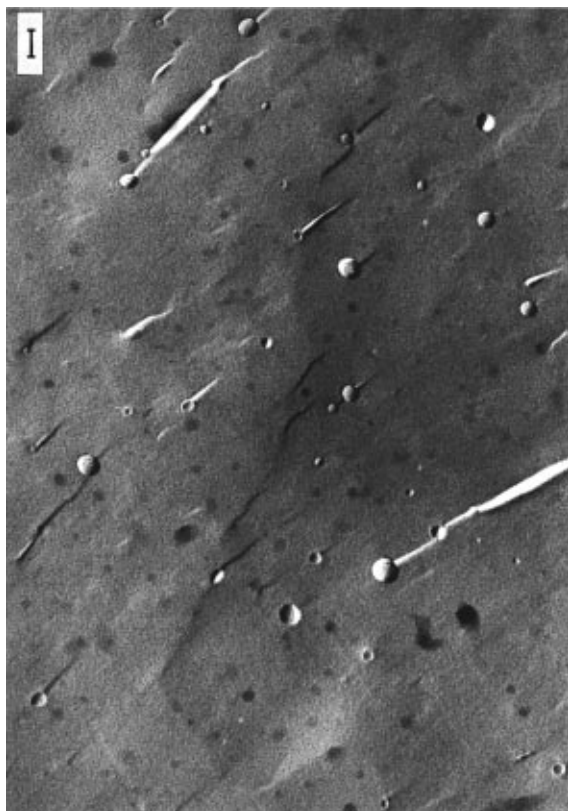


Figure 1. Freeze fracture electron micrograph of DOP-Ade liposomes prepared by means of the extrusion technique. The length of the bar is 100 nm.

relationship^{31,32}

$$\ln(I/I_0) = C\lambda^{-g} \quad (1)$$

where λ is the wavelength, and the exponent g (around 4 for Rayleigh scatterers) and C are parameters that can be adjusted in the fitting procedures. The light scattering curve has been extrapolated to 220 nm and subtracted to the absorption spectrum.

The subtraction is necessary to compare the molar extinction coefficients of spectra of phospholiponucleosides assembled in vesicular structure to those from nucleotides in aqueous solution, which obviously exhibit no scattering.

Results and Discussion

The extrusion of the lipid dispersion produced monodisperse spherical liposomes, as shown in Figure 1 by the freeze fracture EM micrograph of DOP-Ade aggregates.

The liposome shape and size distribution have been further characterized by quasi elastic light scattering, and some results are shown in Figure 2. The autocorrelation function of the light scattered at 90° was analyzed by the cumulant analysis³³ that allowed evaluation of the average hydrodynamic radius of the particles and polydispersity of the sample. The liposomes from DOP-Ade, DOP-Cyt, and DOP-Uri have a 31–33 nm average radius. The hydrodynamic radius remains practically constant over the experimental time scale (see Figure 2), meaning that phospholiponucleosides produce a very stable vesicular dispersion and that light scattering contribution to the UV absorption can be regarded as systematic. A CONTIN analysis^{34,35} of the light scattering data, shown in the inset of Figure 2 for DOP-Uri vesicles, confirms a very narrow size distribution, in accordance with the freeze fracture micrographs.

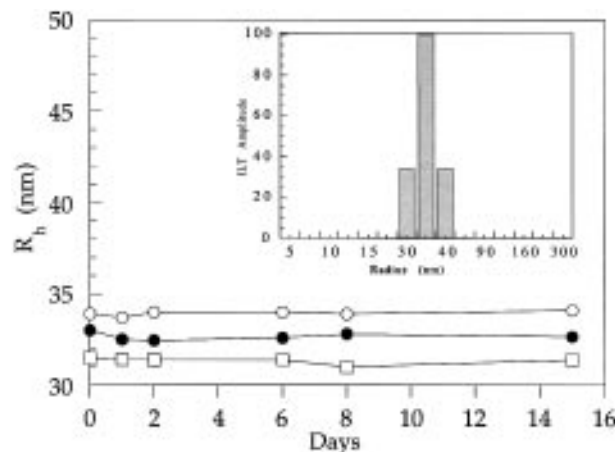


Figure 2. Stability of vesicles from phosphatidynucleosides as determined by quasi elastic light scattering. Vesicles from DOP-Ade (\square), DOP-Uri (\circ), and the 1:1 mixture of the two liposomes populations (DOP-Ade + DOP-Uri) (\bullet). Inset: CONTIN plot for the size distribution of DOP-Uri liposomes.

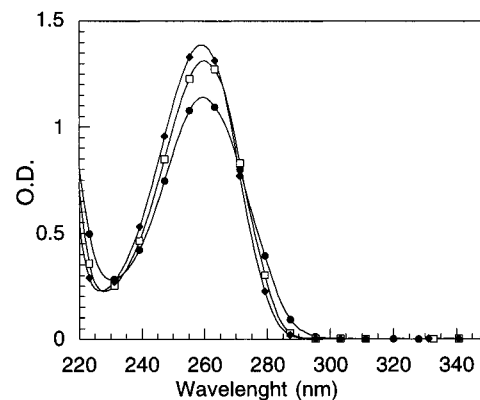


Figure 3. DOP-Ade absorption corrected by subtraction of the light scattering contribution (\bullet), and after the addition of octylglucoside micellar solution (\square), compared to UV absorption of AMP (\blacklozenge).

Liposomes are composed by approximately 21 000 monomers with an internal water pool of about 1.5×10^{-19} L (calculated assuming a molecular area of 139, 125, and 121 Å² for DOP-Ade, DOP-Uri, and DOP-Cyt, respectively, as determined by surface pressure/area isotherms).²³

POP-Ade and POP-Uri vesicles show a small increase of the size of aggregates before the hydrodynamic radius reaches the stable equilibrium value. A similar behavior is observed for liposomes obtained from the mechanical mixture of the same lipids (data not shown).

The comparison of the UV absorption spectra of DOP-Ade and DOP-Uri vesicular solutions with those of adenosine monophosphate and uridine monophosphate shows that no significant change in molar absorption emerges for the DOP-Uri vesicles, whereas a hypochromic effect can be noticed for DOP-Ade vesicles. This observation is consistent with self-stacking of the nucleobases in vesicles, in analogy to the hypochromicity observed for poly(A).^{13,14}

To confirm this hypothesis, we performed the experiment illustrated in Figure 3 for DOP-Ade. Vesicle solutions have been diluted with a defined amount of octylglucopyranoside micellar solution, to a final concentration of 7.5×10^{-4} M for the phospholiponucleoside and 4.5×10^{-2} M for the detergent. This procedure leads to the formation of lipid/detergent mixed micelles, as it is well-known for vesicle-forming phospholipids.³⁶ The collapse of the vesicular structure, confirmed by light scattering measurements, results in an increase of the absorptivity

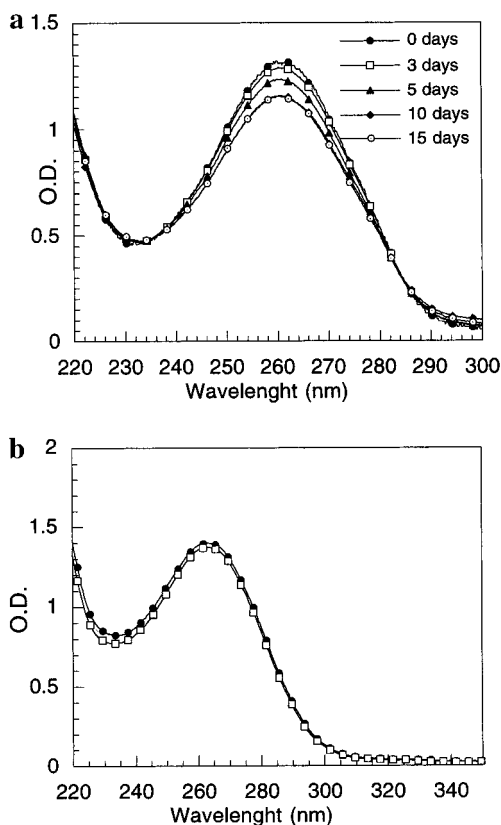


Figure 4. (a) Time dependence of the UV spectra of the mixtures of two complementary vesicle populations, DOP-Ade + DOP-Uri. (b) Time dependence of the UV spectra of the mixtures of two noncomplementary vesicle populations, DOP-Ade + DOP-Cyt. Circles = after mixing, squares = after 15 days.

at 260 nm up to the value of the adenosine monophosphate molecule. This can be readily interpreted as due to a destacking of the phospholiponucleoside headgroups in the mixed micelles.

On the other side, DOP-Uri vesicles do not show hyperchromicity when dissolved in micelles of glucopyranosides to form mixed micelles, probably because the base itself is less hydrophobic and polarizable than adenosine and self-stacking is less favorable. This interpretation is in good agreement with the behavior of the linear polymer poly(U) that fails to give self-stacking.¹⁴

Similar data are available for the POP derivatives: self-stacking is observed only for the POP-Ade and not for the POP-Uri phospholiponucleosides.

These findings support that base–base interactions at the vesicular surface present some characteristics typical of linear polynucleotides, suggesting that the self-assembling properties of phospholipids can replace the sterical support provided by the covalent skeleton in nucleic acids.

As already mentioned, liposomes are stable with respect to shape and size distribution. The spectroscopic features of the samples obtained from pure phospholiponucleosides remain also constant for over 2–3 weeks.

A strikingly different behavior is observed for the spectral properties of the liposomal solutions obtained by mixing phospholiponucleosides vesicles bearing complementary bases. When DOP-Ade vesicles are mixed with DOP-Uri vesicles, the absorbivity at 260 nm decreases slowly with time, as shown in Figure 4a. Since the size distribution of the dispersion remains constant, indicating that no aggregation or fusion is present (Figure 1), the onset of a hypochromic effect can be ascribed

to adenosine–uridine interaction.^{13,15} The absorption band levels off at about 70% of its initial value and stabilizes after some days.

To distinguish between aspecific stacking and Watson–Crick hydrogen-bonding specificity, we have studied the behavior on noncomplementary-base liposomes. Mixtures of the noncomplementary bases DOP-Ade and DOP-Cyt do not show the hypochromic effect found for the complementary phospholiponucleosides (see Figure 4b). Since the average size and the size distribution of the vesicles, monitored by light scattering during the experimental time scale (about 1 month), remain constant, the hypochromicity cannot be ascribed to structural changes of the liposomes. Similar results are obtained with the POP derivatives: in this case a constant plateau in the UV–vis absorption is reached after about 60 h.

It is important to notice that these UV changes obtained at equilibrium are the same as those obtained from the mechanical 1:1 mixture of the two complementary-base lipids, i.e. when the two complementary lipids are first mixed with each other and the mixture is used to prepare liposomes.

The complementarity we have observed supports the hypothesis that the measured hypochromicity is due to a specific interaction between complementary bases and not to hydrophobic interaction among the bases.

The hypochromicity of the UV π – π transition of the bases occurring when DOP-nucleoside or POP-nucleoside vesicles are mixed is coupled to a large increase of intensity of the circular dichroism spectra, as shown in Figure 5a, whereas the CD spectra of the pure component liposomes are comparable to those of adenosine monophosphate and uridine monophosphate (see Figure 5b). The increase of CD intensity has been observed in base-pairing interactions for polynucleotides in solution.^{14,15} Similar results are obtained with the POP derivatives. This increase cannot be observed for DOP-Ade/DOP-Cyt CD spectra, which remain unchanged for over 3 weeks. The time scale of the CD changes occurring upon mixing the two complementary base vesicles is the same as the UV changes. It is important to notice that the plateau value of the molar ellipticity is the same as that obtained from the 1:1 mechanical mixture of the two base lipids (Figure 5a), confirming that by mixing the two complementary base vesicles a stoichiometric base pair has been formed.

The slow time progress of the spectral changes may appear at first surprising. Most likely base recognition is due to a mechanism of lipid exchange between vesicles. In fact, it is well-known that lipid exchange in phosphatidylcholine vesicles is very slow,³⁸ and in the present case the readjusting for base pairing may require an additional slower step.

A temperature increase leads, for the system reported in this study, to a monotonic decrease of the molar ellipticity in the CD spectra of the vesicles in solution. This behavior differs from the classic case of DNA duplexes. In fact, in this case, the increase of temperature induces a denaturation which is readily detected by spectroscopy. The temperature-induced strand separation usually observed in DNA cannot be found in our system, as the separation of the two classes of phosphatidyl nucleosides from the mixed liposomes would correspond to an entropically unfavorable demixing.

Concluding Remarks

The results reported here indicate that base–base interaction is present in liposomes bearing complementary nucleoside structures. Base pairing occurs in a defined liposome shape and size distribution, excluding fusion as the prominent mechanism of liposome interaction. The self-assembling properties

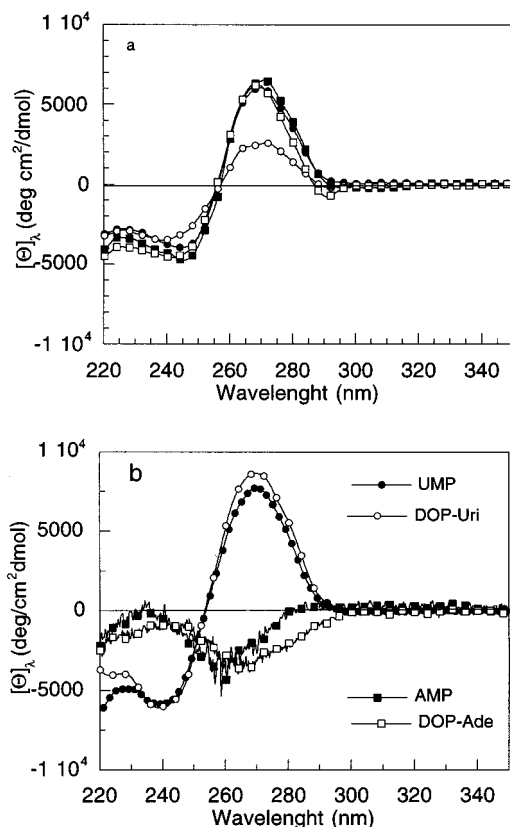


Figure 5. CD spectra of vesicles from phosphatidynucleosides: (a) Time dependence of the CD spectra of a 1:1 mixture of DOP-Ade and DOP-Uridi (DOP-Ade + DOP-Uridi), soon after the preparation (○) and after 2 weeks (□). Comparison with the time evolution of the spectra of vesicles obtained from a 1:1 mixture of the two lipids (DOP-Ade/DOP-Uridi), soon after the preparation (●) and after 2 weeks (■). (b) Comparison of the spectra of vesicles from DOP-Ade (□) and DOP-Uridi (○) with the spectra of the corresponding nucleotides (adenosine monophosphate (■) and uridine monophosphate (●), respectively).

of the lipidic tails provide the nucleosidic moieties with a supramolecular architecture that allows them to form hydrogen bonds. As far as we know, we show for the first time that vesicle organization provides the appropriate environment for base–base recognition in spite of the presence of negatively charged phosphate groups, leading to unfavorable electrostatic interactions, and of the exposure to the aqueous environment, highly competitive for hydrogen bonding.

The spectroscopic properties of the mixture of the complementary liposomes correspond to those of the liposomes obtained from the 1:1 stoichiometric mixture of the two lipids. Since the interaction process is very slow in vesicles, it appears reasonable to conclude that lipid exchange is the main mechanism of the recognition chemistry, allowing complementary base interaction. The result of this process is liposomes containing an average 1:1 composition of the two complementary phosphatidynucleosides.

It is not yet possible to give the molecular details of such a structure. NMR investigations are currently in progress. NMR studies are made difficult by the line broadening caused by the high anisotropy and slow relaxation time of the vesicle structure and the consequent loss of spectral resolution at room temperature.

A working hypothesis that respects all information available is shown in Figure 6. The bases, located at the interface between the lipid layer and the water phase, interact either by hydrogen bonding or stacking interactions. The ribose units, not shown

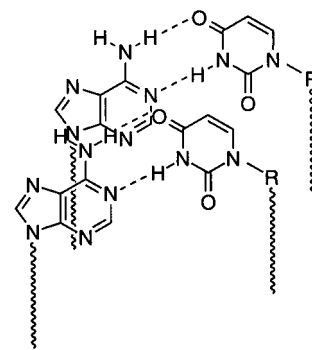


Figure 6. Schematic drawing of the proposed interaction mode.

explicitly, are most probably in contact with the water phase. This drawing, which should be considered for the moment only a working hypothesis, emphasizes complementary base interactions in a lipidic structure.

We mentioned in the Introduction the possible relevance of these compounds and these studies for the origin of life, or more precisely, for the origin of molecular evolution as a route to test a novel pre-RNA world. This study shows that chemical recognition of the bases occurs in a macromolecular structure without covalent bonds among the mononucleotides and in a spherical bilayer lipidic structure, which has often been considered as a good model for a protocell.³⁹ The question is if this composite structure can perform additional functions other than the recognition function shown here. Studies are in progress to assess whether these liposomes may be able to undergo self-reproduction, as it has been shown for other vesicles.⁴⁰ This would then combine, although at a very primitive level, potential information and self-replication. A closely related question is whether the ordered alignment of the nucleoside at the water–oil interface can facilitate their polymerization, as shown for other aligned monolayer systems.⁴¹

Acknowledgment. We are grateful to Michaela Wessicken of the Institute of Polymers at the ETH for the electron microscopy analysis and to Prof. Carlo Bertucci of the Department of Chemistry, University of Pisa, for CD measurements. Thanks are due to MURST, CNR, and “Consorzio per lo sviluppo dei sistemi a grande interfase” (CSGI) for financial support.

Appendix: TLC, NMR, and UV Data

POP-Adenosine. R_f (CHCl₃/MeOH/MeNH₂, 50:30:8): 0.48. UV (CHCl₃/MeOH, 9:1) λ_{\max} = 260 nm.

¹H NMR (DMSO-*d*₆): δ = 0.85 (t, J = 6.4, 6H, CH₃), 1.23 (m, 44H, CH₂ aliphatic), 1.46 (m, 4H, CH₂CH₂COO), 1.96 (m, 4H, CH₂CH=CH), 2.17–2.30 (m, 4H, CH₂–COO), 3.79–3.95 (4H, *sn*-3-CH₂, H5'/5''), 4.03–4.10 (2H, H4', *sn*-1-CH₂), 4.19 (t, 1H, H3'), 4.28 (dd, J_1 = 11.9, J_2 = 2.8, 1H, *sn*-1-CH₂), 4.58 (t, 1H, H2'), 5.07 (m, 1H, *sn*-2-CH), 5.30 (m, 2H, CH=CH), 5.4–5.7 (bs, 2H, 2' OH e 3' OH), 5.92 (d, J = 5.7, 1H, H1'), 7.0–7.5 (bm, 6H, NH₄⁺, NH₂), 8.15 (s, 1H, H2), 8.42 (s, 1H, H8).

¹³C NMR (DMSO-*d*₆): δ = 13.81 (CH₃), 21.99 (CH₂), 24.29 (CH₂CH₂COO), 24.33 (CH₂CH₂COO), 26.47, 26.52 (H₂C–CH=CH), 28.31–31.19 (CH₂), 33.27 (CH₂COO), 33.44 (CH₂–COO), 62.11 (*sn*-1-CH₂), 62.77 (C5'), 64.59 (d, *sn*-3-CH₂), 70.18 (*sn*-2-CH), 70.69 (C3'), 73.74 (C2'), 83.55 (d, C4'), 86.84 (C1'), 118.78 (C5), 129.46 (C=C), 139.24 (C8), 149.49 (C4), 152.35 (C2), 155.8 (C6), 172.13 (C=O), 172.39 (C=O).

³¹P NMR (DMSO-*d*₆): δ = –0.23.

POP-Uridine. R_f (CHCl₃/MeOH/MeNH₂, 50:30:8): 0.33. UV (CHCl₃/MeOH, 9:1) λ_{\max} = 262.5 nm.

¹H NMR (DMSO-*d*₆): δ = 0.85 (t, *J* = 6.8, 6H, CH₃), 1.23 (m, 44H, CH₂ aliphatic), 1.49 (m, 4H, CH₂CH₂COO), 1.97 (m, 4H, CH₂CH=CH), 2.19–2.30 (m, 4H, CH₂COO), 3.74–3.84 (4H, *sn*-3-CH₂, H5'/5''), 3.91 (t, 1H, H2'), 3.98 (t, 1H, H3'), 4.05–4.09 (2H, H4', *sn*-1-CH₂), 4.28 (dd, *J*₁ = 11.9, *J*₂ = 2.9, 1H, *sn*-1-CH₂), 5.06 (m, 1H, *sn*-2-CH), 5.3–5.4 (bm, 4H, CH=CH, 2' OH e 3' OH), 5.55 (d, *J* = 8.1, 1H, H5), 5.78 (d, *J* = 5.6, 1H, H1'), 7.25 (b, 4H, NH₄⁺), 7.87 (d, *J* = 8.1, 1H, H6), 11.27 (b, 1H, NH).

¹³C NMR (DMSO-*d*₆): δ = 13.86 (CH₃), 22.03 (CH₂), 24.36 (CH₂CH₂COO), 24.41 (CH₂CH₂COO), 26.53, 26.57 (H₂CC-H=CH), 28.38–31.25 (CH₂), 33.37 (CH₂COO), 33.54 (CH₂-COO), 62.24 (*sn*-1-CH₂), 62.70 (d, *sn*-3-CH₂), 64.32 (d, C5'), 70.31 (*sn*-2-CH), 70.38 (C3'), 73.33 (C2'), 83.41 (d, C4'), 87.56 (C1'), 101.73 (C5), 129.51, 129.54 (C=C), 140.74 (C6), 150.74 (C2), 162.99 (C4), 172.19 (C=O), 172.46 (C=O).

³¹P NMR (DMSO-*d*₆): δ = -0.09.

DOP-Cytidine. *R*_f(CHCl₃/MeOH/MeNH₂, 50:40:1): 0.65. UV (CHCl₃/MeOH, 9:1): λ_{\max} = 276 nm.

¹H NMR (DMSO-*d*₆): δ = 0.90 (t, 6H, CH₃), 1.30 (m, 40H, CH₂ aliphatic), 1.60 (m, 4H, CH₂CH₂COO), 2.05 (m, 8H, CH₂-CH=CH), 2.40 (m, 4H, CH₂COO), 3.90 (m, 4H, H5'/5''), *sn*-3-CH₂, 4.00 (m, 1H, H4'), 4.05 (m, 2H, H2', H3') 4.20 (m, 1H, *sn*-1-CH₂) 4.40 (dd, 1H, *sn*-1-CH₂), 5.18 (m, 1H, *sn*-2-CH), 5.35 (m, 1H, 3' OH), 5.40 (m, 5H, 2' OH, CH=CH), 5.70 (d, 1H, H5), 5.90 (d, 1H, H1'), 7.2 (bm, 4H, NH₄⁺), 7.43 (s, 2H, NH₂), 8.00 (d, 1H, H6).

¹³C NMR (DMSO-*d*₆): δ = 14.21 (CH₃), 23.04 (CH₂), 25.32 (CH₂CH₂COO), 27.56 (H₂CCH=CH), 29.58–32.26 (CH₂), 34.48 (CH₂COO), 34.62 (CH₂COO), 63.02 (*sn*-1-CH₂), 64.06 (*sn*-3-CH₂), 64.14 (C5'), 69.30 (C3'), 70.91 (d, *sn*-2-CH), 75.67 (C2'), 83.49 (d, C4'), 91.03 (C1'), 95.58 (C5), 130.12 (HC=CH), 130.38 (HC=CH), 143.69 (C6), 155.86 (C2), 165.24 (C4), 174.02 (C=O), 174.44 (C=O).

³¹P NMR (DMSO-*d*₆): δ = 1.02.

DOP-Adenosine. *R*_f(CHCl₃/MeOH/MeNH₂, 50:40:1): 0.67. UV (CHCl₃/MeOH, 9:1) λ_{\max} = 262 nm.

¹H NMR (DMSO-*d*₆): δ = 0.90 (t, 6H, CH₃), 1.30 (m, 40H, CH₂ aliphatic), 1.60 (m, 4H, CH₂CH₂COO), 2.05 (m, 8H, CH₂-CH=CH), 2.35 (m, 4H, CH₂-COO), 3.92 (t, 2H, *sn*-3-CH₂), 4.00 (m, 2H, H5'/5''), 4.14 (q, 1H, H4'), 4.17 (dd, 1H, *sn*-1-CH₂), 4.30 (t, 1H, H3'), 4.39 (dd, 1H, *sn*-1-CH₂), 4.69 (t, 1H, H2'), 5.18 (m, 1H, *sn*-2-CH), 5.40 (m, 4H, CH=CH), 5.60 (bs, 2H, 2' OH e 3' OH), 6.00 (d, 1H, H1'), 7.3 (bm, 4H, NH₄⁺), 7.41 (s, 2H, NH₂), 8.15 (s, 1H, H2), 8.59 (s, 1H, H8).

¹³C NMR (DMSO-*d*₆): δ = 13.84 (CH₃), 21.99 (CH₂), 24.31 (CH₂CH₂COO), 24.33 (CH₂CH₂COO), 26.47, 26.50 (H₂CC-H=CH), 28.34–31.09 (CH₂), 33.27 (CH₂COO), 33.42 (CH₂-COO), 62.17 (*sn*-1-CH₂), 62.75 (C5'), 64.59 (d, *sn*-3-CH₂), 70.18 (*sn*-2-CH), 70.72 (C3'), 73.74 (C2'), 83.48 (d, C4'), 86.88 (C1'), 118.85 (C5), 129.46 (C=C), 139.27 (C8), 149.59 (C4), 152.49 (C2), 155.92 (C6), 172.22 (C=O), 172.48 (C=O).

³¹P NMR (DMSO-*d*₆): δ = -0.69.

DOP-Uridine. *R*_f(CHCl₃/MeOH/MeNH₂, 50:40:1): 0.66. UV (CHCl₃/MeOH, 9:1) λ_{\max} = 263 nm.

¹H NMR (DMSO-*d*₆): δ = 0.90 (t, 6H, CH₃), 1.30 (m, 40H, CH₂ aliphatic), 1.60 (m, 4H, CH₂CH₂COO), 2.05 (m, 8H, CH₂-CH=CH), 2.35 (m, 4H, CH₂COO), 3.87 (t, 2H, *sn*-3-CH₂), 3.91 (m, 2H, H5'/5''), 4.01 (bq, 1H, H4'), 4.10 (t, 1H, H3'), 4.17 (bt, 1H, H2'), 4.19 (dd, 1H, *sn*-1-CH₂), 4.40 (dd, 1H, *sn*-1-CH₂), 5.18 (m, 1H, *sn*-2-CH), 5.35 (bs, 1H, 3' OH), 5.40 (m, 4H, CH=CH), 5.50 (bs, 1H, 2' OH), 5.70 (d, 1H, H5), 5.90 (d, 1H, H1'), 7.1 (bs, 4H, NH₄⁺), 7.90 (d, 1H, H6), 11.40 (s, 1H, NH).

¹³C NMR (DMSO-*d*₆): δ = 13.87 (CH₃), 22.00 (CH₂), 24.36 (CH₂CH₂COO), 24.41 (CH₂CH₂COO), 26.50, 26.56 (H₂CC-H=CH), 28.39–31.05 (CH₂), 33.37 (CH₂COO), 33.54 (CH₂-COO), 62.24 (*sn*-1-CH₂), 62.68 (d, *sn*-3-CH₂), 64.34 (d, C5'), 70.31 (*sn*-2-CH), 70.37 (C3'), 73.33 (C2'), 83.39 (d, C4'), 87.55 (C1'), 101.74 (C5), 129.52, 129.63 (C=C), 140.81 (C6), 150.76 (C2), 163.02 (C4), 172.22 (C=O), 172.48 (C=O).

³¹P NMR (DMSO-*d*₆): δ = -0.33.

References and Notes

- (1) Katz, L.; Penman, S. *J. Mol. Biol.* **1966**, *15*, 220.
- (2) Hamlin, R. M., Jr.; Lord, R. C.; Rich, A. *Science* **1966**, *148*, 173.
- (3) Pitha, J.; Pithova, P. *Can. J. Chem.* **1966**, *44*, 1405.
- (4) L. Williams, G. W.; Williams, L. D.; Shaw, B. R. *J. Am. Chem. Soc.* **1989**, *111*, 7205.
- (5) Pranata, J.; Wierschke, S. G.; Jorgensen, W. L. *J. Am. Chem. Soc.* **1991**, *113*, 2810.
- (6) Pistolis, G.; Paleos, C. M.; Malliaris, A. *J. Phys. Chem.* **1995**, *99*, 8896.
- (7) Saenger, W. *Principles of Nucleic Acid Structure*; Springer-Verlag: New York, 1984.
- (8) Cantor, C. R.; Shimmel, P. R. *Biophysical Chemistry*; W. H. Freeman and Co.: San Francisco, 1980.
- (9) Freifelder, D. *Physical Biochemistry*; W. H. Freeman and Co.: San Francisco, 1982.
- (10) Nielsen, P. E. *Orig. Life Evol. Biosph.* **1993**, *23*, 323.
- (11) Lehn, J. M. *Angew. Chem. Int. Ed. Engl.* **1988**, *27*, 90.
- (12) Ringsdorf, H.; Schlarb, B.; Venzmer, J. *Angew. Chem.* **1988**, *100*, 117.
- (13) Fendler, J. H. *Membrane Mimetic Chemistry*; Wiley: New York, 1982.
- (14) Lehn, J. M. *Supramolecular Chemistry*; VCH: Weinheim, 1995.
- (15) Fuhrhop, J.-H.; Köning, J. *Membranes and Molecular Assemblies: The Synergetic Approach*; The Royal Society of Chemistry: Cambridge, 1994.
- (16) Novick, J. S.; Chen, J. S.; Noronha, G. *J. Am. Chem. Soc.* **1993**, *115*, 7636.
- (17) Honda, Y.; Kurihara, K.; Kunitake, T. *Chem. Lett.* **1991**, 681.
- (18) Kawahara, T.; Kurihara, K.; Kunitake, T. *Chem. Lett.* **1992**, 1839.
- (19) Berndt, P.; Kurihara, K.; Kunitake, T. *Langmuir* **1995**, *11*, 3083.
- (20) Ahlers, M.; Ringsdorf, H.; Rosemeyer, H.; Seela, F. *Colloid Polym. Sci.* **1990**, *268*, 132.
- (21) Onda, M.; Yoshihara, K.; Koiano, H.; Ariga, K.; Kunitake, T. *J. Am. Chem. Soc.* **1996**, *118*, 8254.
- (22) Bonaccio, S.; Wessicken, M.; Berti, D.; Walde, P.; Luisi, P. L. *Langmuir* **1996**, *12*, 4976.
- (23) Berti, D.; Franchi, L.; Luisi, P. L.; Baglioni, P. *Langmuir* **1997**, *13*, 3438–3444.
- (24) Shuto, S.; Ueda, S.; Imamura, S.; Fukukawa, K.; Matsuda, A.; Ueda, T. *Tetrahedr. Lett.* **1987**, *28*, 199.
- (25) Shuto, S.; Ito, H.; Ueda, S.; Imamura, S.; Fukukawa, K.; Tsujino, M.; Matsuda, A.; Ueda, T. *Chem. Pharm. Bull.* **1988**, *36*, 209.
- (26) Shuto, S.; Imamura, S.; Fukukawa, K.; Ueda, T. *Chem. Pharm. Bull.* **1988**, *36*, 5020.
- (27) Bonaccio, S. Liposomen aus Phosphatidyl nucleosiden, Diss. ETH Nr. 11232, Zürich, 1995.
- (28) Bonaccio, S.; Walde, P.; Luisi, P. L. *J. Phys. Chem.* **1994**, *98*, 6661.
- (29) Shaka, A. J.; Freeman, R. *J. Magn. Reson.* **1983**, *51*, 169.
- (30) Mueller, M.; Meister, N.; Moor, H. *Mikroskopie* **1980**, *36*, 129.
- (31) Barrow, D. A.; Lentz, B. R. *Biochim. Biophys. Acta* **1980**, *597*, 92.
- (32) Franses, E. I.; Talmon, Y.; Scriven, L. E.; Davis, H. T.; Miller, W. G. *J. Colloid Interface Sci.* **1982**, *86*, 449.
- (33) Koppel, D. E. *J. Chem. Phys.* **1972**, *57*, 4814.
- (34) Provencher, S. W.; Hendrix, J.; De Maeyer, L.; Paulussen, N. *J. Chem. Phys.* **1978**, *69*, 4273.
- (35) Provencher, S. W. *Macromol. Chem.* **1979**, *180*, 201.
- (36) Lasic, D. D. *Liposomes: From Physics to Applications*; Elsevier: Amsterdam, 1993.
- (37) Curtis Johnson, W. In *Circular Dichroism: Principles and Application*; Nakanishi, K.; Berova, N.; Woody, R. J., Eds.; VCH: New York, 1994.
- (38) Jones, J. D.; Thompson, T. E. *Biochemistry* **1989**, *28*, 129.
- (39) Morowitz, H. J.; Heinz, B.; Deamer, D. W. *Origins Life Evol. Biosphere* **1988**, *18*, 281.
- (40) Vonmont-Bachmann, P. A.; Luisi, P. L.; Lang, J. *Nature* **1992**, *357*, 57.
- (41) Bader, H.; Dorn, K.; Hupfer, B.; Ringsdorf, H. *Adv. Polym. Sci.* **1985**, *64*, 1.